GOES-R Advanced Baseline Imager Color Product Development

DONALD W. HILLGER

NOAA/NESDIS/StAR/RAMMB, Fort Collins, Colorado

(Manuscript received 31 August 2006, in final form 30 October 2007)

ABSTRACT

The current Geostationary Operational Environmental Satellite (GOES) series was inaugurated in 1994 with the launch of *GOES-8* and will continue with two more satellites (GOES-O and -P) after the most recent *GOES-13* launched in 2006. The next-generation GOES (beginning with GOES-R) will be launched in the 2015 time frame. This new series of satellites will include improved spatial, temporal, spectral, and radiometric resolution. The last two characteristics are manifest by an increased number of spectral bands and increased precision for measurements from those bands. To take advantage of the lead time needed to design, build, and test this new and complex satellite system, work is going into developing image products to be implemented as soon as GOES-R becomes operational.

Preparations for GOES-R image products for applications to various weather events, especially mesoscale events, are well underway. The approach used for these "risk reduction" activities is to apply data from existing operational and experimental satellites (both polar orbiting and geostationary) to create image products that will emulate those to be available from GOES-R as closely as possible. Those image products can either be new products or improvements leveraged on existing operational products. In this article, the new GOES-R Advanced Baseline Imager is briefly reviewed, and the evolutionary development of two qualitative products—one for the detection of fog and stratus, and the other for blowing dust—is presented. Emphasis is on the evolutionary development of these mesoscale products and possible quantitative discrimination among the various image features that are seen.

1. Introduction

An extensive effort is being undertaken to work toward new and improved products that will be available for application when the Geostationary Operational Environmental Satellite (GOES)-R is launched in the 2015 time frame. Some of the initial product development work has already been reported in preliminary form (Hillger et al. 2004a,b,c; Hillger and DeMaria 2007), with focus on product development for the Advanced Baseline Imager (ABI). Not only can existing products be improved because of the increased (spatial, temporal, spectral, and radiometric) resolutions of the ABI, but new products can be developed that would not have been possible from the selection of bands from the current GOES imager and sounder.

To emulate the GOES-R ABI bands (Table 1), various existing satellite imagery is being utilized. In particular, the experimental imagery from the polar-orbiting Earth Observation System (EOS) *Terra* and *Aqua* Moderate Resolution Imaging Spectroradiometer (MODIS) instruments cover all but two of the spectral bands that will be available on the ABI (Table 2). MODIS has 36 bands, but product development work is focused in this article on the ABI-equivalent MODIS bands only, those that will be available operationally on future GOES-R, rather than all available MODIS bands.

In addition, operational real-time geostationary imagery from the Meteosat Second Generation (MSG) satellite is used to produce experimental products. Although not as many spectral bands are shared between the MSG Spinning Enhanced Visible and Infrared Imager (SEVIRI) and ABI (Table 3), there is an advantage with MSG data in that products developed from geostationary data can be observed as they change over time. The time dimension adds motion to certain image features such as clouds to help distinguish clouds from surface-based image features that do not move. Surface observations are used for verification of the ability to detect and discriminate among the various image fea-

Corresponding author address: Donald W. Hillger, Ph.D., NOAA/NESDIS/StAR/RAMMB, CIRA/Colorado State University, Fort Collins, CO 80523-1375.
E-mail: hillger@cira.colostate.edu

DOI: 10.1175/2007JTECHA911.1

TABLE 1. GOES-R ABI bands and bandwidths.

ABI band	Central wavelength (μm)	Wavelength range (μm)	Band explanation	Spatial resolution (km) at nadir
1 (blue)	0.47	0.45–0.49	Visible/reflective	1
2 (red)	0.64	0.59–0.69	Visible/reflective	0.5
3	0.865	0.846–0.885	Reflective	1
4	1.378	1.371–1.386	Cirrus	2
5	1.61	1.58–1.64	Snow/ice	1
6	2.25	2.225–2.275	Particle size	1
7	3.90	3.80–4.00	Shortwave IR window	2
8	6.19	5.77–6.6	Water vapor	2
9	6.95	6.75–7.15	Water vapor	2
10	7.34	7.24–7.44	Water vapor	2
11	8.5	8.3–8.7	Water vapor, SO_2	2
12	9.61	9.42–9.8	Ozone	2
13	10.35	10.1–10.6	Longwave IR window	2
14	11.2	10.8–11.6	Longwave IR window	2
15	12.3	11.8–12.8	Longwave IR	2
16	13.3	13.0–13.6	Longwave IR	2

tures. However, there is usually limited spatial coverage of such ground truth information for verification.

In the sections below some of the important factors to be considered in the selection of spectral bands, as well as suggested methodologies to be used in developing new or improved image products, are outlined. Also important is the use of three-color techniques to detect and enhance image features of interest and to discriminate those features from the many other atmospheric and surface features that are common in most satellite images. As examples of new or improved products, section 2 will focus on the development of a new daytime fog and stratus product; and section 3 will likewise focus on a new blowing-dust product. Section 4 will summarize what has been learned about band and color selection in the examples of product development used in this study, as well plans for the future of the current product development efforts.

2. Fog/stratus product development

An initial focus of the image product development work for GOES-R is an improved fog and stratus product. Stratus (or *stratiform* cloud, as might be more

TABLE 2. Comparison of 16-band GOES-R ABI with EOS MODIS bands (all at 1-km spatial resolution or better).

GOES-R ABI		MODIS	
Band No.	Central wavelength (μm)	Band No.	Central wavelength (μm)
1 (blue)	0.47	3 (blue)	0.47
2 (red)	0.64	1 (red)	0.64
3	0.86	2	0.86
4	1.38	26	1.38
5	1.61	6	1.64
6	2.26	7	2.13
7	3.9	22	3.96
8	6.15	No equivalent	No equivalent
9	7.0	27	6.7
10	7.4	28	7.3
11	8.5	29	8.55
12	9.7	30	9.7
13	10.35	No equivalent	No equivalent
14	11.2	31	11.0
15	12.3	32	12.0
16	13.3	33	13.3

TABLE 3. Comparison of 16-band GOES-R ABI with MSG SEVIRI bands (all at 3-km spatial resolution).

GOES-R ABI		MSG SEVIRI	
Band No.	Central wavelength (μm)	Band No.	Central wavelength (μm)
1 (blue)	0.47	No equivalent	No equivalent
2 (red)	0.64	1 (red)	0.635
3	0.86	2	0.81
4	1.38	No equivalent	No equivalent
5	1.61	3	1.64
6	2.26	No equivalent	No equivalent
7	3.9	4	3.92
8	6.15	5	6.25
9	7.0	No equivalent	No equivalent
10	7.4	6	7.35
11	8.5	7	8.7
12	9.7	8	9.66
13	10.35	No equivalent	No equivalent
14	11.2	9	10.8
15	12.3	10	12.0
16	13.3	11	13.4

proper terminology) is defined for this article as low- to middle-level cloud with little vertical development, composed mainly of *water drops* (as opposed to cirrus cloud, composed mainly of *ice crystals*). Fog is defined as cloud *on or near the ground*, composed of water drops.

Work on this product is focused mainly on qualitatively detecting/discriminating fog and stratus, especially during the daytime, from many other features in satellite imagery, such as clouds containing ice crystals, various land and water surface types, as well as snow cover and ice on the land. Some additional extension of this effort is aimed at quantitatively discriminating fog (on or near the ground) from stratus (low- to middle-level cloud). It will be shown that the new product has this quantitative ability because of the use of multispectral imagery. That ability will be explored further in future applications and real-time testing that are planned.

A widespread fog case identified with the help of the Portland, Oregon, National Weather Service (NWS) Office is used as the first example of the new daytime fog/stratus product. That case at 1910 UTC 11 February 2005 (daytime) contained many different types of clouds, as well as both snow-covered and snow-free land surfaces. (In addition, another daytime view was examined for this particular case study, as well as two nighttime views. However, only the daytime cases have the visible bands available to generate the proposed daytime fog/stratus product.) This case study will be examined through a brief history of products used for fog/stratus detection/discrimination, leading to a new daytime fog/stratus product, utilizing the strengths of the new spectral bands that will become available on GOES-R.

a. Fog/stratus product history

The current state of the art for fog/status detection from GOES is the two-part *fog/reflectivity product* (Dills et al. 1996) that has long proven useful for detecting/discriminating fog/stratus from ice clouds and land and water surfaces because of the lower emissivity (more properly called "emittance"), or higher reflectivity (albedo), of water droplets compared to ice crystals in the shortwave window band at 3.9 μm. The two parts of the fog/reflectivity product are the nighttime fog product and the daytime reflectivity product, which are combined at the day/night terminator to create a single fog/stratus product.

At night for the fog/stratus product, the shortwave window-band brightness (or radiative) temperature is subtracted from the longwave window-band (10.7 μm) temperature to qualitatively discriminate low emissivity (high albedo) clouds from other features in the imagery (Ellrod 1995). The Ellrod technique is the basis for the fog product used at the National Oceanic and Atmospheric Administration (NOAA)/National Environmental Satellite, Data, and Information Service (NESDIS) Operational Product Development Branch, with the image products displayed on the Web (available at http://www.orbit.nesdis.noaa.gov/smcd/opdb/aviation/fog.html). The fog/stratus product is produced preferentially at night, because the same fog/stratus surfaces that have low emissivity at night have high reflectivity during the day. Reflected solar energy from fog/stratus masks the lower temperatures in the shortwave IR band, making the fog/stratus product discrimination of fog/stratus from other image features not as good.

The daytime reflectivity product is combined with the nighttime fog/stratus product to discriminate fog/stratus from other clouds during the day. The reflectivity product, which also effectively subtracts the shortwave and longwave bands, converts that temperature difference into a radiance related to the albedo of various image features, such as the more reflective low- to middle-level water droplet clouds. This image product has been used at the Cooperative Institute for Research in the Atmosphere (CIRA) since the development of the Regional and Mesoscale Meteorology (RAMM) Advanced Meteorological Satellite Demonstration and Interpretation System (RAMSDIS; Molenar et al. 2000) in the 1990s. The reflectivity product is used routinely by NOAA's Satellite Applications Branch as one of the image products used for volcanic ash detection at the Washington, D.C., Volcanic Ash Advisory Center (VAAC). [See information online at (http://www.ssd.noaa.gov/VAAC/aleut.html) for the reflectivity product used for the Aleutian Islands Volcano Watch.]

A further, more recent improvement over the fog/reflectivity product is the *shortwave albedo product* (Kidder et al. 2000). The product computes the shortwave albedo of various cloud and land surfaces by determining the reflected component of the shortwave window-band radiance. This is the *isotropic* albedo, because it does not take into account bidirectional effects; that is, it is the albedo if the scene were an isotropic reflector, one that reflects uniformly in all directions. The pertinent equations for the shortwave albedo from that reference are reproduced below.

The radiance $L_{3.9}$ measured by the satellite at 3.9 μm can be written as the sum of the emitted and reflected radiation,

$$L_{3.9} = (1 - A_{3.9})B_{3.9}(T_{10.7}) + \pi^{-1}A_{3.9}B_{3.9}(T_{\text{sun}})\Omega_{\text{sun}}\cos\zeta, \quad (1)$$

where $B_{3.9}(T_{10.7})$ represents the 3.9-μm radiance that the satellite would measure if there were no solar reflection (based on the temperature at 10.7 μm), and $A_{3.9}$ is the shortwave albedo. The last term is the solar irradiance of the scene at 3.9 μm (based on solar temperature T_{sun} of 5888 K at 3.9 μm), where Ω_{sun} is the solid angle of the sun subtended at the earth (6.8×10^{-5} sr), and ζ is the solar zenith angle.

Solving (1) for the albedo $A_{3.9}$ yields

$$A_{3.9} = \frac{L_{3.9} - B_{3.9}(T_{10.7})}{\pi^{-1} B_{3.9}(T_{\text{sun}}) \Omega_{\text{sun}} \cos\zeta - B_{3.9}(T_{10.7})}. \quad (2)$$

In other words, the shortwave albedo is computed by subtracting the emitted radiance at 3.9 μm, using the temperature from the longwave window band (10.7 μm), from the total radiance at 3.9 μm. During the day, the albedo is the shortwave radiance surplus (more than the emitted radiance alone) for solar-reflective surfaces. For those same surfaces at night there is a shortwave radiance deficit (less than the emitted radiance if the emissivity were unity). Whether positive or negative, the albedo, or inversely the emissivity, is a characteristic of land and cloud surfaces independent of whether the sun is shining. Using (2), the shortwave albedo product is generated, day or night, with the additional feature that the albedo is corrected to a nadir view through the cosine correction for solar zenith angle. This increases the brightness (or intensity) of off-nadir image pixels so that they appear as if the sun were directly overhead.

The shortwave albedo product is the starting point for developing a new daytime fog/stratus product for GOES-R. For the daytime case study being examined, the shortwave albedo product, as generated from MODIS shortwave and longwave window bands, is shown in Fig. 1a. World Meteorological Organization (WMO) weather symbols from surface observations for the hour before (1900 UTC) and the hour after (2000 UTC) the image time are plotted on the image to indicate areas of fog (F), haze (H), and ground fog (GF). In this product, highly reflective water droplet clouds are white, and less reflective ice crystal clouds and land surfaces are generally darker. This product detects fog and stratus well, which appear white or in lighter shades, and discriminates fog/stratus from land surfaces and ice clouds, all of which appear as various darker shades. Fog and stratus are discriminated to some degree from each other, partly by brightness and otherwise by the texture of the clouds in the product. The fog has "lower relief" to the earth's surface, compared to stratus, which has edges or shadows, suggesting the elevated low- to middle-level nature of those stratiform clouds compared to fog (on or near the ground).

b. The role of three-color imagery

Because of the wider selection of bands that will be available with GOES-R ABI, one of the ways to utilize the various bands is through three-color [red, green, and blue (RGB)] compositing.[1] Color compositing is now widely available with most image processing systems, in contrast to the much more limited use of the color processing of meteorological satellite imagery nearly 20 yr ago, as demonstrated by d'Entremont and Thomason (1987), when they used a fog case as one of their examples of the three-color technique. Much more recently, RGB analysis appears to be the focus of most of the best-practice product development for multispectral MSG imagery as presented by J. Kerkmann et al. (2005, unpublished manuscript; available online at http://oiswww.eumetsat.org/WEBOPS/msg_interpretation/PowerPoints/Channels/rgbpart04_20050420.ppt). See the appendix to this article for an explanation of the algorithm/software developed and used to generate the three-color images and image loops for this study.

As an example of an RGB product, one of the most user-friendly RGB products created from MSG imagery is called a "natural" color product. Based on MSG heritage bands, this product is a composite of MODIS-equivalent bands at 1.6, 0.8, and 0.6 μm for the red, green, and blue components, respectively. Figure 1b is an example of the natural color product for the same fog/stratus case and with the same weather symbols featured in Fig. 1a. In this product, lower- to middle-level and highly reflective water droplet clouds are white, less reflective ice crystal clouds and snow-covered ground are cyan, and land surfaces are either green or brown, depending on the amount of vegetative ground cover. The land surface vegetation discrimination is due to the 0.8-μm green band, whereas the discrimination between water and ice cloud is due to the 1.6-μm snow/ice band (Rosenfeld et al. 2004; Eastwood and Thyness 2003). This product detects/discriminates fog and stratus from other image features, such as land surfaces and ice clouds. An advantage of this product, over that of the shortwave albedo, is that the use of color helps discriminate among several image features, more than just fog and stratus (water cloud) from other land and cloud surfaces.

[1] RGB compositing means *true* color analysis only when the RGB bands are the red, green, and blue colors, respectively, of the visible spectrum; otherwise, the RGB compositing is called three color or false color when the bands are not those of the natural color spectrum.

(a)

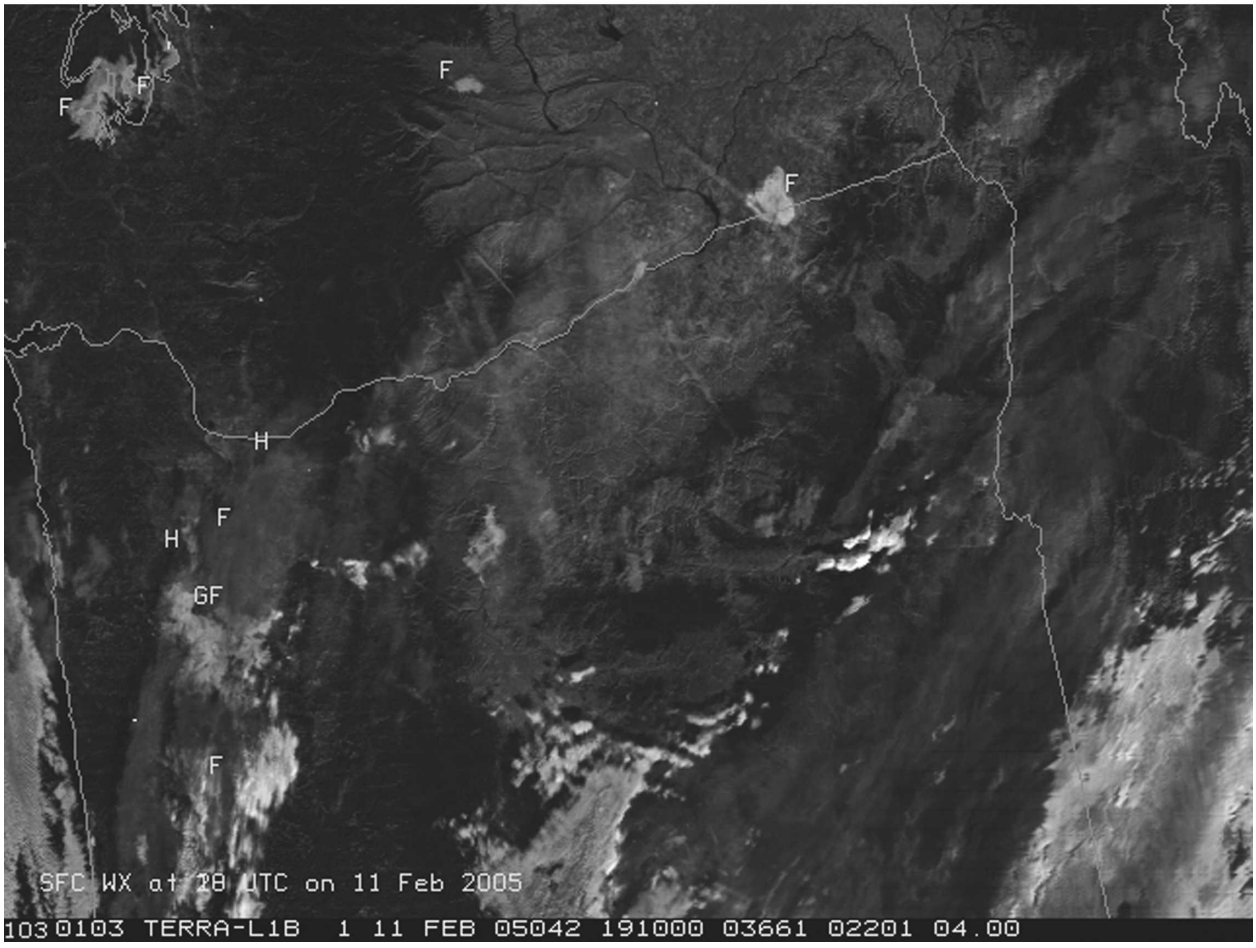

Fig. 1. (a) Shortwave albedo product generated from MODIS shortwave and longwave IR bands showing patches of fog and stratus in southern Washington and northern Oregon at 1910 UTC 11 Feb 2005 (daytime). WMO weather symbols from surface observations for the hour before (1900 UTC) and the hour after (2000 UTC) the image time are plotted on the image to indicate areas of fog (F), haze (H), and ground fog (GF). Fog and stratus (middle-level water clouds) are white/light, whereas ice clouds and most land surfaces are dark. (b) MSG heritage natural three-color product, but generated from equivalent MODIS bands, showing patches of fog and stratus, as well as snow-covered and snow-free ground, for the same scene and with the same weather symbols as in (a). Snow cover and ice clouds are cyan, low clouds are white, vegetated land surfaces are green, and nonvegetated land is brown. (c) New daytime fog/stratus three-color product, generated from MODIS imagery, which better discriminates clouds from land, and between different levels and types of clouds, for the same scene and along with the same weather symbols as in (a) and (b). Snow-covered ground is red; high-level cirrus/ice clouds are orange; lower- to middle-level stratus/water clouds are white with a blue tint; fog (on or near the ground) is white with a yellow tint, and most land surfaces are green.

c. Modifying an existing MSG RGB product for a new daytime fog/stratus product

The next step in the development of a new fog/stratus product is to take advantage of existing MSG techniques for fog/stratus detection/discrimination. An RGB product used to discriminate fog/stratus from snow cover during the day utilizes the 0.8-, 1.6-, and 3.9-μm bands (J. Kerkmann et al. 2005, unpublished manuscript; available online at http://oiswww.eumetsat.org/WEBOPS/msg_interpretation/PowerPoints/Channels/rgbpart04_20050420.ppt). In this snow/fog product all three of the MSG bands are nonlinearly adjusted (by raising the normalized values to a power of 1/1.7) before combining the images to emphasize lower (deemphasize higher) values in the range of the image brightness. Also, the 3.9-μm band is the solar/reflected part only. The emitted part of the shortwave band is removed, similar to the way the shortwave albedo product is computed, before combining it with the other bands in the RGB composite. Because the shortwave albedo product contains most of the signal or explained

(b)

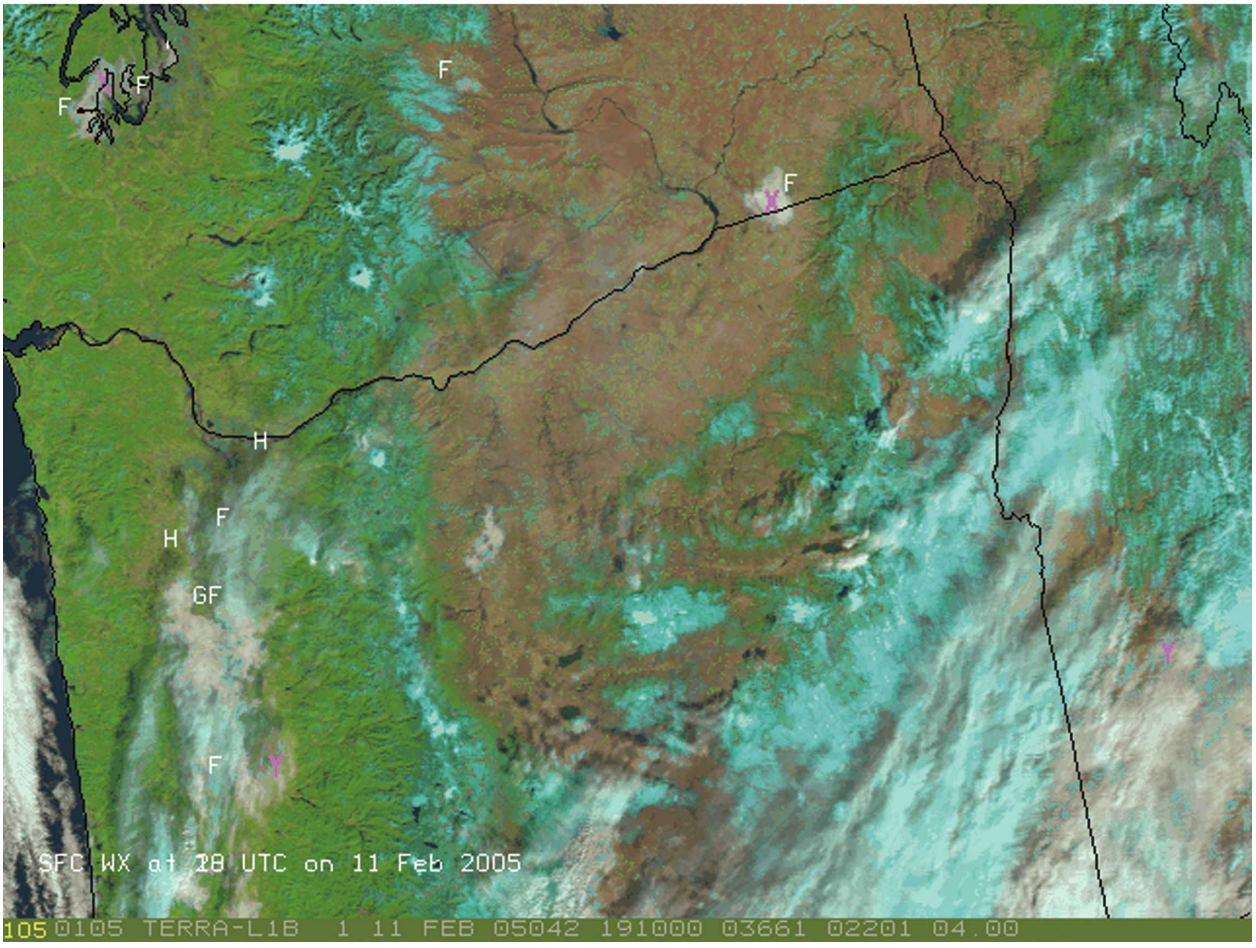

Fig. 1. (*Continued*)

variance in fog/stratus discrimination, it becomes the primary input for evolving a new daytime fog/stratus product.

The 1.6-μm band is also a prime contributor to the MSG fog product because of the large difference in ice/water reflectivity at this wavelength. Therefore, this band was selected as a second input for use in the new daytime fog/stratus product to help discriminate snow cover and ice from other image features.

However, the third component of the current MSG daytime snow/fog product has been changed to the 0.6-μm (red) band instead of the green band at 0.8 μm, which is a band that is available on many satellite-based land remote sensing instruments to discriminate surfaces that are covered by vegetation. This sacrifices the discrimination of differently vegetated land surfaces, allowing more color variation for cloud level and type, variations that are harder to otherwise distinguish from each other without the use of color.

Another feature of the new RGB fog/stratus composite is that the two reflective bands (0.6 and 1.6 μm) are enhanced first by applying an albedo correction. This correction adjusts the image brightness, compensating for nonnadir solar zenith angles, by dividing image radiances by the cosine of the zenith angle, as was similarly done for the shortwave albedo (2). This process is outlined by Kidder et al. (2000), and is called the *visible albedo product* when applied to visible band radiances. (As with the shortwave albedo, this product is an *isotropic* albedo, which assumes that surfaces being viewed reflect uniformly in all directions, because the angular reflection properties of what is being viewed are not known.) This processing is used instead of the nonlinear image adjustments that are applied to these bands in the MSG-equivalent product. The MSG snow/fog product has not been recreated for this case; only the new fog/stratus product is shown next.

Figure 1c shows the new daytime fog/stratus product

(c)

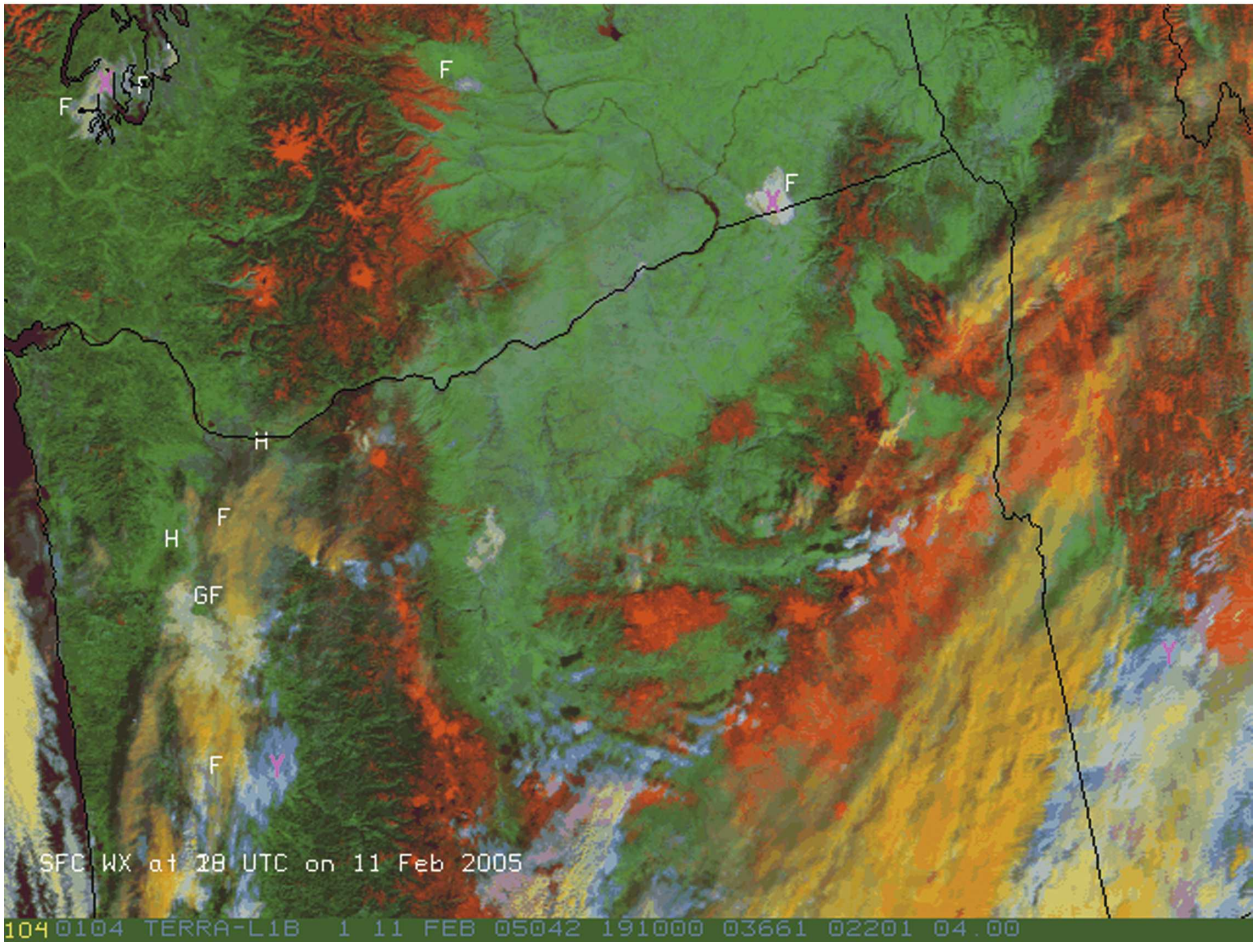

Fig. 1. (*Continued*)

based on the current MSG daytime snow/fog product, but modified as noted above and applied to equivalent MODIS bands for the same scene and with the same weather symbols as in Figs. 1a,b. Of the three products shown, this product better discriminates clouds from land and between different levels and types of clouds. The better use of contrasting colors, compared to the natural color product, helps discriminate various features in the image.

Table 4 explains the colors in the three-color product that appear for various types of features such as snow cover, cirrus, stratus, fog, and land surfaces. The colors of the features were not predicted before the product was created; rather, they are explained by looking at the relative magnitudes of the radiance contributions from the red, green, and blue components. Although the RGB component images are not all shown, the contributions are summarized as follows: Snow-covered areas in the image are red because snow has high reflectivity (low emissivity) in the visible (red) band, whereas snow-covered surfaces have low reflectivity (high emissivity) in the near-IR 1.6-μm (green) band and the shortwave 3.9-μm albedo (blue). High-level cirrus/ice clouds are orange because both the visible (red) and near-IR (green) bands have higher radiance contributions than the shortwave albedo (blue). Equal mixtures of red and green would produce yellow, but the orange color comes from a higher contribution from the visible (red) image. Stratus/water (low to middle level) clouds are mainly white with a blue tint; and fog (on or near the ground) is white with a yellow tint. The ability to differentiate between fog and stratus relied mostly on texture differences and shadows noted in the shortwave albedo product previously discussed. In this color product, both fog and stratus have medium contributions from the visible (red) and near-IR (green) bands, but a low contribution from the shortwave albedo (blue). The variation in tint between fog and stratus (blue ver-

TABLE 4. Relative magnitudes of radiance contributions to three-color daytime fog/stratus product.

Image feature	Red component (0.6-μm albedo)	Green component (1.6-μm albedo)	Blue component (3.9-μm albedo)	Resulting color
Snow	High	Low	Low	Red
Cirrus	High	Medium	Low	Orange
Stratus	Medium	Medium	High	White/blue tint
Fog	Medium	Medium	High	White/yellow tint
Land	Low	High	Medium	Green

sus yellow) is likely due to subtle differences in the magnitudes of the contributions from the shortwave (blue) and visible (red) bands. These subtle differences in solar absorption and reflection are magnified by the three-color combination product. (More about the discrimination between fog and stratus will be noted in the next subsection.) Finally, most land surfaces are green because of the higher contribution of the near-IR (green) band compared to the contributions from the visible (red) band and shortwave albedo (blue).

d. Quantitative discrimination of fog versus stratus

A first cut at quantifying the discrimination between fog (on or near the ground) and stratus (low to middle level) cloud between the two products in Figs. 1b,c is presented in Fig. 2. Scatterplots in each of the four panels indicate where all image pixels (over 30 000 pixels total in each image) lay in RGB space, by comparing the RGB components two at a time. Units in these plots are the 8-bit counts (0–255) that are input to the three-color RGB processing, but they represent the radiances in the respective RGB components as indicated in Table 4. The upper two plots compare the red versus green (upper left) and green versus blue (upper right) components, respectively, for the new fog/stratus product. The lower two plots compare the red versus blue (lower left) and red versus green (lower right) components for the natural color product used as a baseline for color product improvement. In all four panels, pixels identified as fog in Fig. 1c (white with a yellow tint) are marked yellow, and pixels identified as stratus (white with a blue tint) are marked cyan, compared to all other pixels in magenta. Fog and stratus pixels were taken at 225 (15×15) pixels at two locations each, marked by Xs and Ys respectively, in Fig. 1c. Both upper plots, derived from the new fog/stratus product in Fig. 1c, indicate discrimination between fog and stratus pixels, whereas the same fog versus stratus pixels overlap and are not distinct in both lower plots derived from the natural color product in Fig. 1b. Appropriate thresholds could be generated from these types of plots to identify all fog versus stratus pixels based on either or both of the upper plots from the new fog/stratus product.

e. Another fog/stratus case and two-case summary

In addition to the first case study, used in the development of the new daytime fog/stratus product, a second case over the central valley of California at 2120 UTC 11 January 2004 is shown in Fig. 3. This case, which also contains many different types of cloud and land surfaces, including cirrus over low- to middle-level clouds, was analyzed using the same three-color RGB combination as the first fog/stratus case (in Fig. 1c). Various image features are nicely discriminated by the same colors noted in Table 4 for the previous example: fog is white with a yellow tint, low- to middle-level stratus/water clouds are white with a blue tint, land surfaces are green, snow cover is red, and cirrus/ice clouds are orange.

Table 5 summarizes the three-color image combinations in the evolution of the new daytime fog/stratus product being developed in the previous paragraphs. The new three-color fog/stratus product is currently being produced in real time, every 15 min, from MSG imagery over Europe on an experimental RAMSDIS unit at CIRA. As an example of this product, a time series image loop of the daytime fog/stratus product is displayed (see online at http://rammb.cira.colostate.edu/intranet/Weeklies/Hillger060811MSGfog/loop.html, which can be compared to the shortwave albedo product, online at http://rammb.cira.colostate.edu/intranet/Weeklies/Hillger060811MSGSW/loop.html, and/or compared to the MSG natural color product, online at http://rammb.cira.colostate.edu/intranet/Weeklies/Hillger060811MSGnatural/loop.html). In this example, the new daytime fog/stratus product better discriminates between various types and levels of cloud, as well as surface features, than the other products from which it was derived. Eventual real-time loops will be available as time permits.

With the new daytime fog/stratus product as an example of product development for ABI, it is important

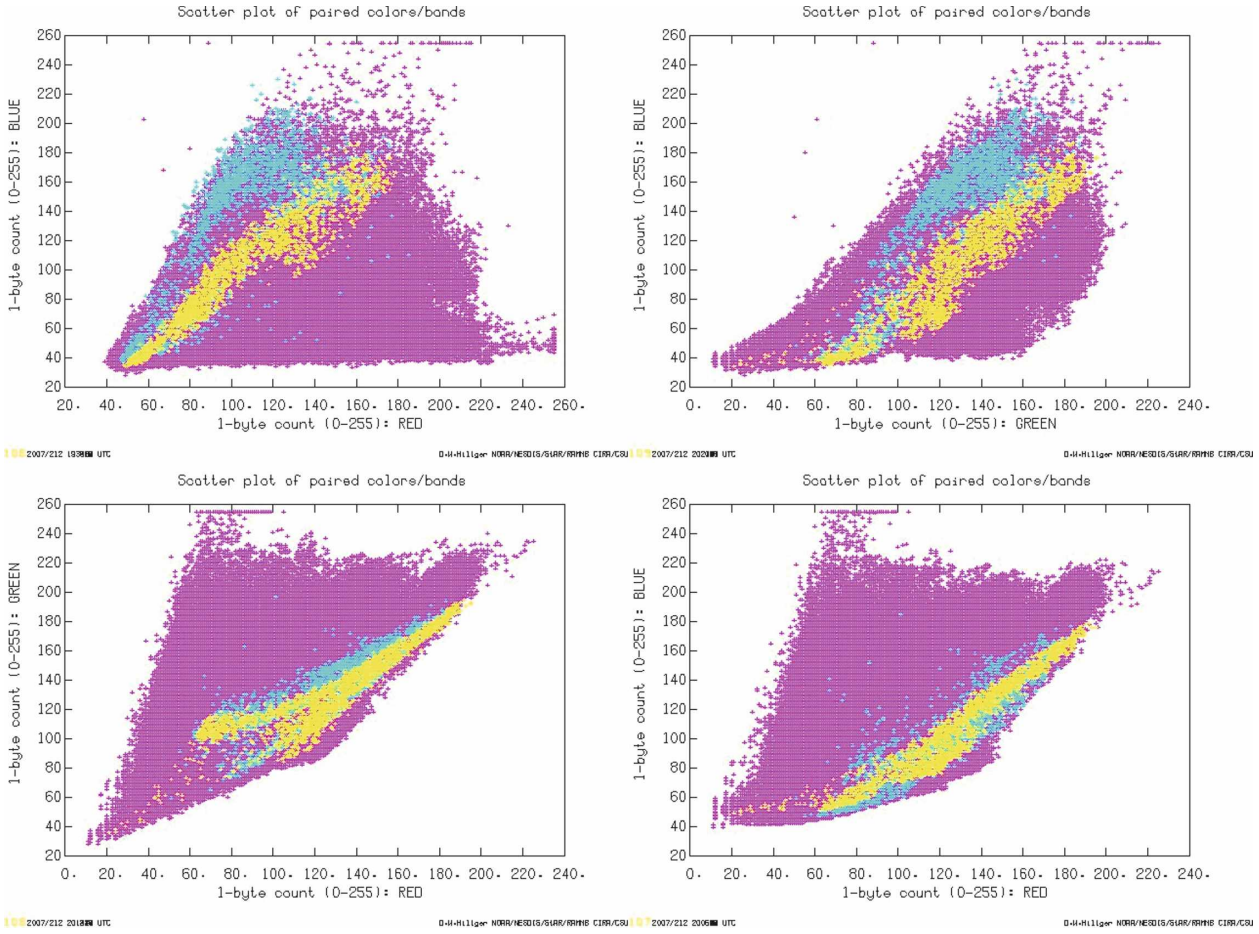

FIG. 2. Scatterplot comparison of image pixels identified as fog (yellow) vs stratus (cyan) vs all other image pixels (magenta). Fog and stratus pixels were taken at two locations each, marked by Xs and Ys respectively, in Fig. 1c. (top) Comparison derived from the new fog/stratus product indicate discrimination between fog and stratus, whereas (bottom) the same pixels overlap and are not distinct when derived from the natural color product.

to summarize at this point some of the constraints and product heritage that can be used in product evolution. Those constraints include choosing the ABI-equivalent bands that will be available with future GOES-R instrumentation, as well as utilizing existing imagery from both MODIS and MSG. In addition, techniques used in heritage fog/stratus products are leveraged and utilize three-color techniques widely applied to MSG data.

3. Blowing-dust product development

In addition to fog and stratus, another area of interest for product development is in the detection of blowing dust. As with the fog/stratus product, as a starting point for a qualitative blowing-dust product, MSG three-color product development is used as a guide, while taking into consideration the ABI-equivalent MSG bands that will be available on future GOES-R.

A good atmospheric dust product that is generated operationally can be seen on the Eumetsat Image Gallery Web site (online at http://www.eumetsat.int/Home/Main/Image_Gallery/Derived_Product_Imagery/index.htm?l=en; with an Eumetsat product generation description online at http://oiswww.eumetsat.int/~idds/html/product_description.html). The dust product, generated from MSG bands at 8.7, 10.8, and 12.0 μm, has been attributed to D. Rosenfeld (2006, personal communication). However, the use of these particular "trispectral" bands can be traced back to the work of Strabala et al. (1994) for use in cirrus cloud detection. The same bands were extended for use with blowing dust over water and land by Ackerman (1997) and evaluated (over water) for MSG/SEVIRI by Brindley and Russell (2006).

An example of this blowing-dust product is shown in Fig. 4 as applied to equivalent MODIS bands for a dust

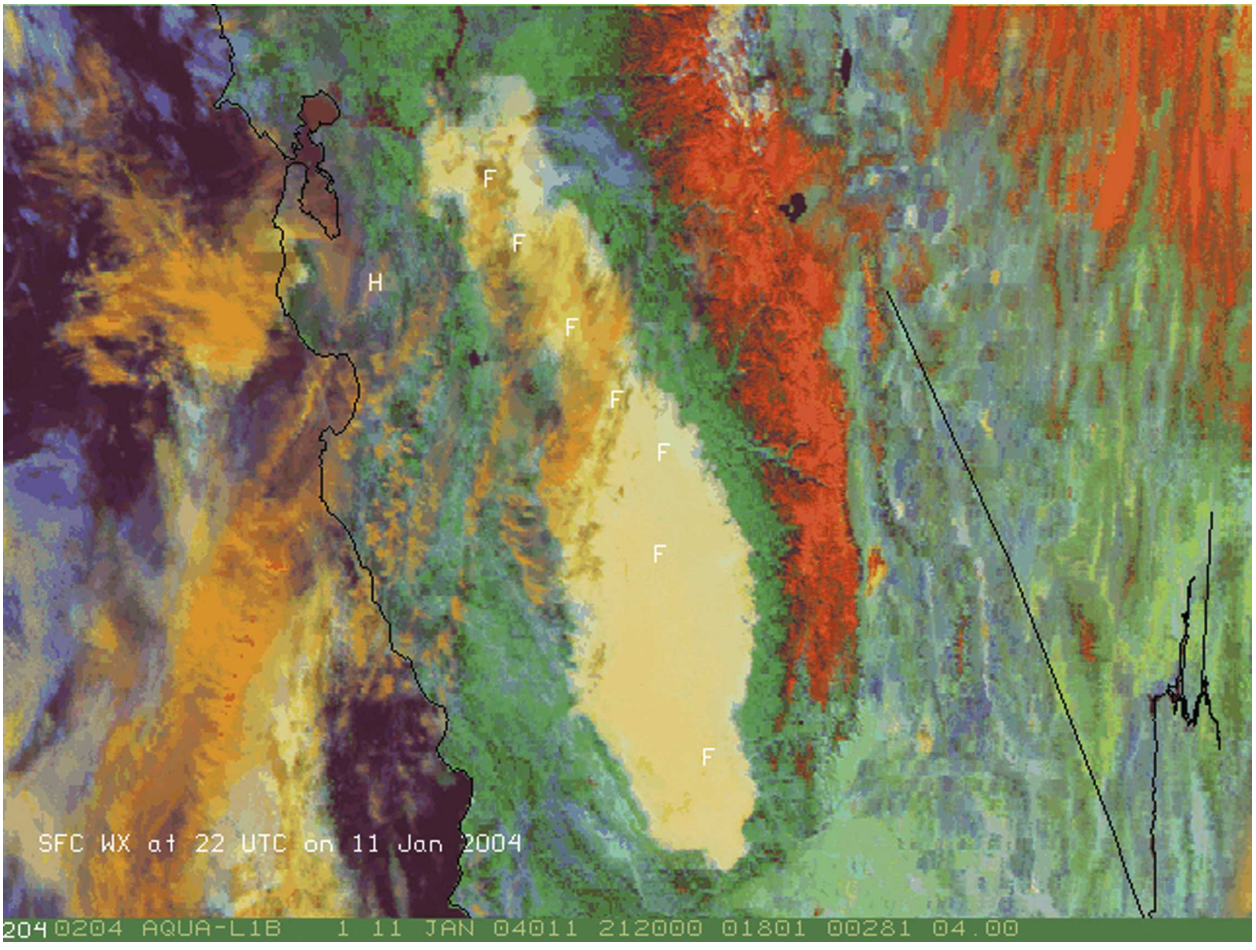

FIG. 3. Same as Fig. 1c, but for a second case of fog/stratus in the central valley of California at 2120 UTC 11 Jan 2004. WMO weather symbols from surface observations for the hour after (2200 UTC) the image time are plotted on the image to indicate areas of fog (F) and haze (H). Fog is again white with a yellow tint, low- to middle-level stratus/water clouds are white with a blue tint, land surfaces are green, snow-covered ground is red, and cirrus/ice clouds are orange.

case over the high plains of eastern Colorado and western Kansas and Nebraska at 1930 UTC 18 April 2004. Note the magenta-colored airborne dust, immediately surrounded by blue for clear skies, along with yellow, rust, and black for clouds.

To verify the dust feature, WMO weather symbols from surface observations locations are plotted (in black) on the image in Fig. 4 for several hours before the image time and (in white) for a few hours after the event. Symbols in the vicinity of the blowing dust indicate haze (∞) rather than dust, as well as at downwind stations for later times (in white). Because of the scar-

TABLE 5. Summary of three-color image combinations for daytime fog/stratus detection/discrimination.

Three-color product name	Red component	Green component	Blue component	Image example
MSG natural three-color product	1.6 μm	0.86 μm	0.6 μm	Fig. 1b
MSG "day snow/fog" three-color product	0.8 μm*	1.6 μm*	3.9 μm (solar/reflected part only)*	Not shown
Modified three-color fog/stratus product	0.6-μm albedo**	1.6-μm albedo**	Shortwave (3.9 μm) albedo**	Fig. 1c

* The counts in these bands are nonlinearly adjusted (by raising the normalized values to a power of 1/1.7) before being combined (J. Kerkmann et al. 2005, unpublished manuscript; available online at http://oiswww.eumetsat.org/WEBOPS/msg_interpretation/PowerPoints/Channels/rgbpart04_20050420.ppt).

** The solar zenith angle–corrected isotropic albedo at each pixel.

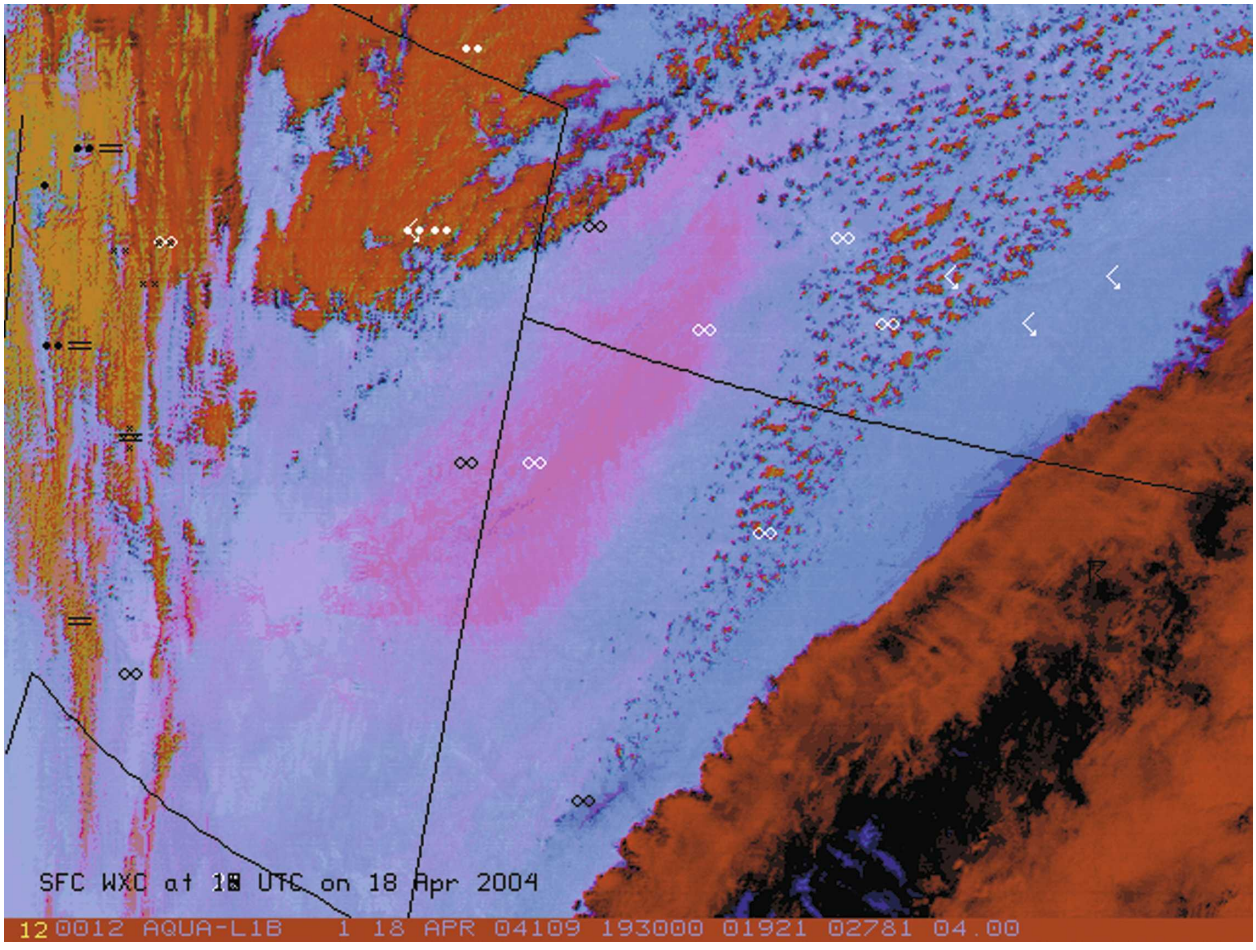

FIG. 4. Three-color MSG heritage atmospheric dust product for a case of blowing dust over eastern Colorado and western Kansas and Nebraska at 1930 UTC 18 Apr 2004. The product is generated from the ABI-equivalent MODIS bands at 8.7, 10.8, and 12.0 μm. Airborne dust is magenta colored, immediately surrounded by a clear-sky background in blue, along with clouds in yellow, rust, and black. Composited weather symbols for the area indicate haze (∞).

city of surface reporting stations in this area, the image product gives a much better indication of the spatial extent and varying density of the airborne dust than the surface observations. The lack of conventional observations for verification is not uncommon compared to the much higher spatial resolution satellite-derived products. Similarly, a three-color dust visualization technique developed by Miller (2003) compares the dust cloud to that seen in enhanced visible imagery to illustrate the improved ability to detect dust in cases where surface observations are almost nonexistent.

In an attempt to improve on the dust product given as a starting point, the same three spectral bands were processed via principal component image (PCI) analysis (Hillger and Ellrod 2003), a technique that can be applied to multispectral imagery in order to extract spectral difference information to detect many types of atmospheric phenomena that are generally better detected by band-differencing techniques. PCI analysis reorders the signal in the bands into principal components in terms of the amount of explained variance. PCI analysis of a set of spectral bands results in an equal number of PCIs, with common/redundant information in the first PCI and spectral difference information in the other higher-order PCIs.

PCI analysis was chosen as an image improvement or enhancement technique for the *infrared* images for dust cases that are examined in this study, similar to the choice of the albedo enhancement for *visible* images in the fog discrimination cases. Whereas PCIs can be applied to visible imagery as well as infrared imagery, or to a combination of visible and infrared bands, an albedo enhancement is not an option for infrared imagery, leaving PCIs as a way to extract spectral difference information from imager bands that otherwise contain a significant portion of redundant information.

(a)

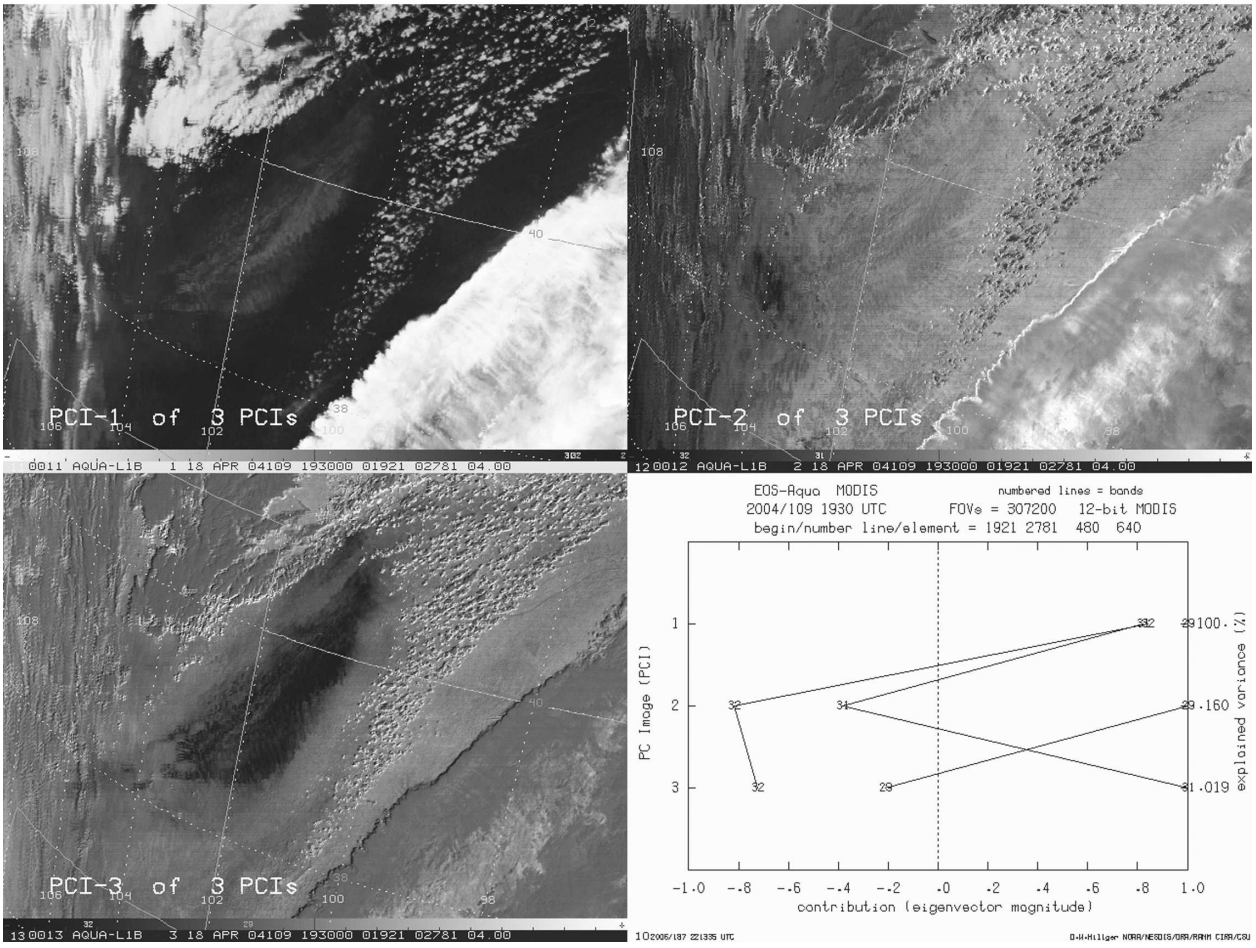

Fig. 5. (a) Four-panel image of three PCIs generated from ABI-equivalent MODIS bands at 8.7, 10.8, and 12.0 μm, plus a plot of the MODIS band makeup of the three PCIs, for the same case as in Fig. 4. (b) Three-color atmospheric dust product generated from PCI-2, -3, and -1 (red, green, and blue, respectively) in (a), showing dust as red, immediately surrounded by a clear-sky background in yellow/orange. Note also the area in green near the source of the dust plume. Clouds are blue and pink.

The results of PCI analysis are shown as panels in Fig. 5a, generated from the three MODIS bands that were input, along with a plot of the band makeup of the three PCIs (in the lower-right corner). This last panel shows how the MODIS bands are combined for PCI-1, -2, and -3. PCI-1 (read horizontally across the graph) is a positive weighted mean of the three MODIS bands, and appears similar (upper-left corner) to any of the input bands because they contain largely redundant information. PCI-2 and -3 are sums and differences the three input bands with weights indicated in the plot. Note that the largest dust signal, compared to image background, occurs in PCI-3, an image mainly composed of the "split window" difference between MODIS longwave IR bands 31 (10.8 μm) and 32 (12.0 μm), with a much smaller contribution from somewhat shorter-wavelength band 29 (8.7 μm). The longwave IR difference, the major component of PCI-3 in this case, is known to be a good indicator of airborne dust from previous work (Hillger and Ellrod 2003). The dust plume also has a signal in PCI-1, because this PCI contains information from all of the bands that were input. However, in PCI-2 the dust signal is almost completely absent, except for a dark area near the source of the dust plume. Because PCI-2 is mainly the difference between the longwave IR bands and the 8.7-μm band, that difference is likely due to emissivity differences between these wavelengths, possibly related to vegetation or land surface differences in this area.

As an additional step, three-color techniques can then be applied to the PCIs, resulting in the proposed blowing-dust product in Fig. 5b. All color combinations of the three PCIs were tried, with the dust being more clearly distinct from other features in the resulting

(b)

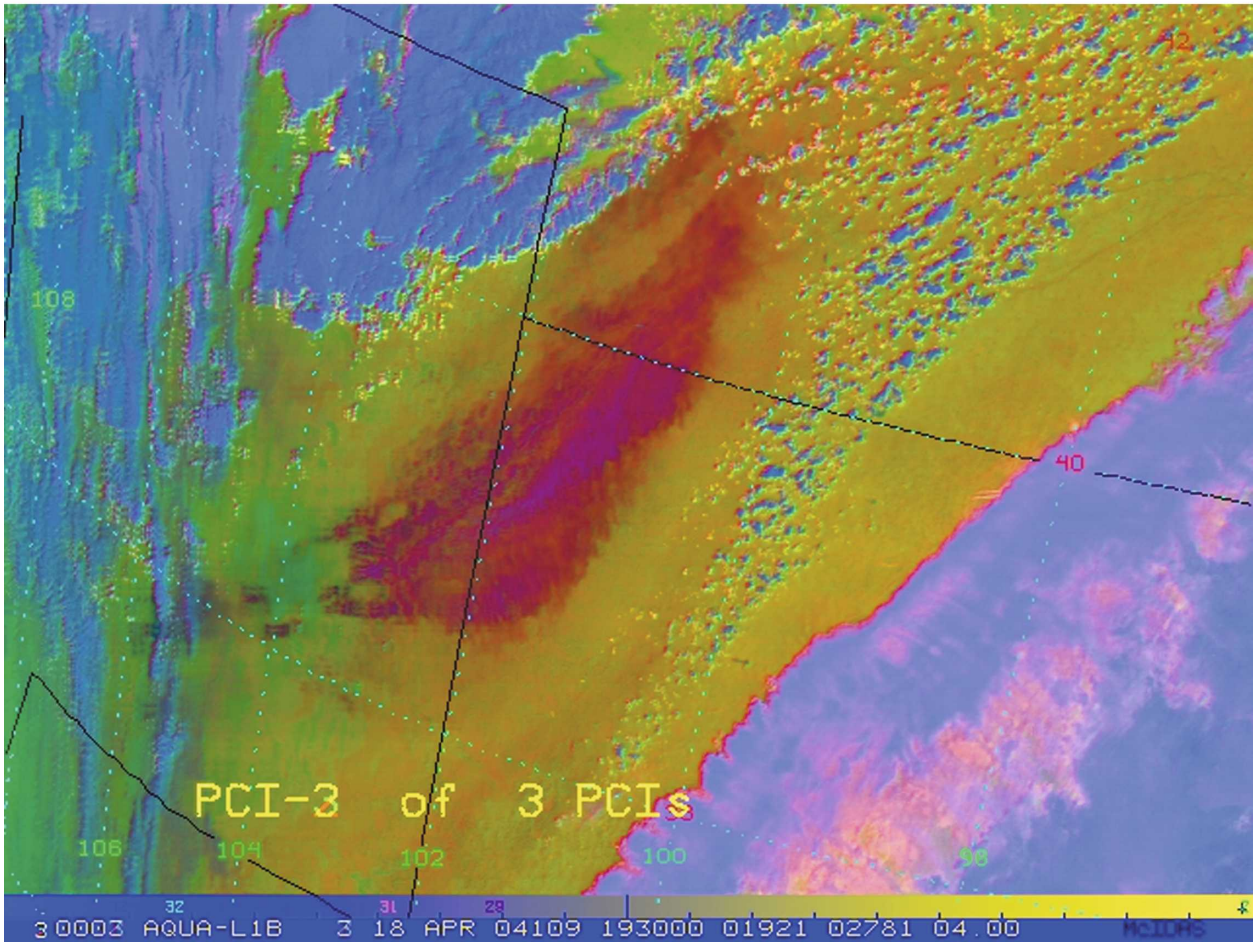

Fig. 5. (*Continued*)

three-color image when the red, green, and blue colors are applied to PCI-2, -3, and -1, respectively. In this chosen combination, airborne dust is red, immediately surrounded by a clear-sky yellow/orange background.

The upper part of Table 6 gives the relative magnitudes of brightness (intensity) contributions of the three PCIs to the three-color blowing-dust product. Because dust is the feature of interest, the color of the dust and its color contrast to other image features is of primary concern, and not necessarily the colors of most of the other features. In this case the red color for blowing dust arises from a medium to high contribution from PCI-2 (red), a low contribution from PCI-3 (green), and a medium to low contribution from PCI-1 (blue). It is interesting that the red color is assigned to PCI-2, which does not show the blowing dust, yet the dust appears to be red because of the low contributions from the green and blue components (PCI-3 and PCI-1, respectively), which show the dust plume. An important principle of color combinations is at work in this case, an outcome that would not easily be predicted without experimenting with the various color combinations.

Note also the area in green near the source of the dust plume, identified in PCI-2, with the major part of the dust plume starting downwind of that feature. For this feature the medium contribution from the green component, compared to the low contributions from the red and blue components, makes this feature green. Finally, clouds are blue and pink. This three-color image product clearly detects and discriminates dust from surrounding clear sky and cloud. However, is an even better image combination possible?

An attempt to answer that question leads to the addition of the MODIS 3.9-μm band to the other three bands. As basis for using this band, Ackerman (1989) indicates that this shortwave band is best utilized during the day, but nighttime application is also possible. The additional band is available on MODIS and will be

TABLE 6. Relative magnitudes of brightness contributions to three-color blowing-dust product: three-PCI case.

Image feature	Red component (PCI-2 of three PCIs)	Green component (PCI-3 of three PCIs)	Blue component (PCI-1 of three PCIs)	Resulting color
Blowing dust	Medium to high	Low	Medium to low	Red
Dust source region	Low	Medium	Low	Green
		Four-PCI case		
Image feature	Red component (PCI-2 of four PCIs)	Green component (PCI-4 of four PCIs)	Blue component (PCI-3 of four PCIs)	Resulting color
Blowing dust	High	Low	Low	Red
Dust source region	Medium	Medium	Low	Orange

available with GOES-R. It also was chosen because it is a window band that can sense lower-atmospheric features. With four input bands, PCI analysis results in four PCIs shown as panels in Fig. 6a, where the dust plume appears in all four panels to some degree. The makeup of three of the PCIs (PCI-1, -3, and -4) in Fig. 6b is similar to that produced in the three-band analysis, but additional information arises from the 3.9-μm band mainly in PCI-2. In the PCI-2 image (upper-right corner) the higher concentrations of blowing dust appear white, but with not as much emphasis on the spatial extent of the dust. For the other components, the makeup of PCI-3 and -4 are similar to PCI-2 and -3, respectively, in the three-band/three-PCI case.

Most three-color combinations of the four-PCI case were tried, with many more possibilities to choose both PCIs and colors than for the three-PCI case. One of the combinations deemed to be best is shown in Fig. 6c. (Again, the best combination was determined by the ability to discriminate dust from other atmospheric and land surface features, as well create a color combination that especially highlights the dust plume. The color selection process is *subjective*, in that other good color combinations are possible, but the chosen combination is based on what should work well for image interpretation.) The chosen product is a combination of PCI-2, -4, and -3 (for the red, green, and blue colors, respectively), with good emphasis on the dust plume in contrast to most of the other image features.

The lower part of Table 6 gives the relative magnitudes of brightness contributions of the three-of-four selected PCIs to the three-color blowing-dust product. The red signal for the blowing dust is due to the high contribution from PCI-2 compared to the low contributions from PCI-4 and -3 (green and blue, respectively). This is the case, in spite of the fact that PCI-4 shows the spatial extent of the dust better than the other PCIs. What PCI-2 adds is sensitivity to higher concentrations of blowing dust. That sensitivity comes from the added 3.9-μm band, the major contributor to PCI-2, and the opposite is from the contributions of the longer wavelength bands, as seen in Fig. 6b.

The dust source region in this combination is orange compared to the other more neutral-colored pixels near the dust plume. The medium but unequal contributions from PCI-2 and -4 (red and green, respectively) compared to the low contribution from PCI-3 (blue) results in the orange color, rather than yellow, which would be produced by equal contributions from red and green.

Clouds and most other image features in Fig. 6c are represented by more suppressed/neutral colors. In that sense this product is an improvement over that of the dust product in Fig. 4, the three-band/three-PCI dust product. Plotted winds on the image (representing the magnitude and direction of the flow at surface observation locations at the time) help verify that the spatial extent and elongated orientation of the blowing dust is reasonable. This is especially important when there are few observing stations and even fewer reports of the actual dust plume, an increasing occurrence as surface observations become more automated.

Another dust case and two-case summary

In addition to the first study, a second blowing-dust case for the Texas Panhandle and western Oklahoma at 1940 UTC 6 April 2006 is shown in Fig. 7. For this case, the dust covers a very large area and includes some range fires and smoke. Using four-band/four-PCI analysis, like that used for the first case (in Fig. 6c), the band contributions to the PCIs and resulting colors in the final product are very similar, even with the PCIs recalculated for this new case. (Alternately, a fixed set of PCIs with fixed band contributions may be used for multiple images, provided that neither the input bands nor the scene changes radically, rather than recalculating the PCIs for each image. This will result in less variation between product images when combined into an image loop.)

In Fig. 7 various image features are nicely discriminated from each other, with dust represented again by

(a)

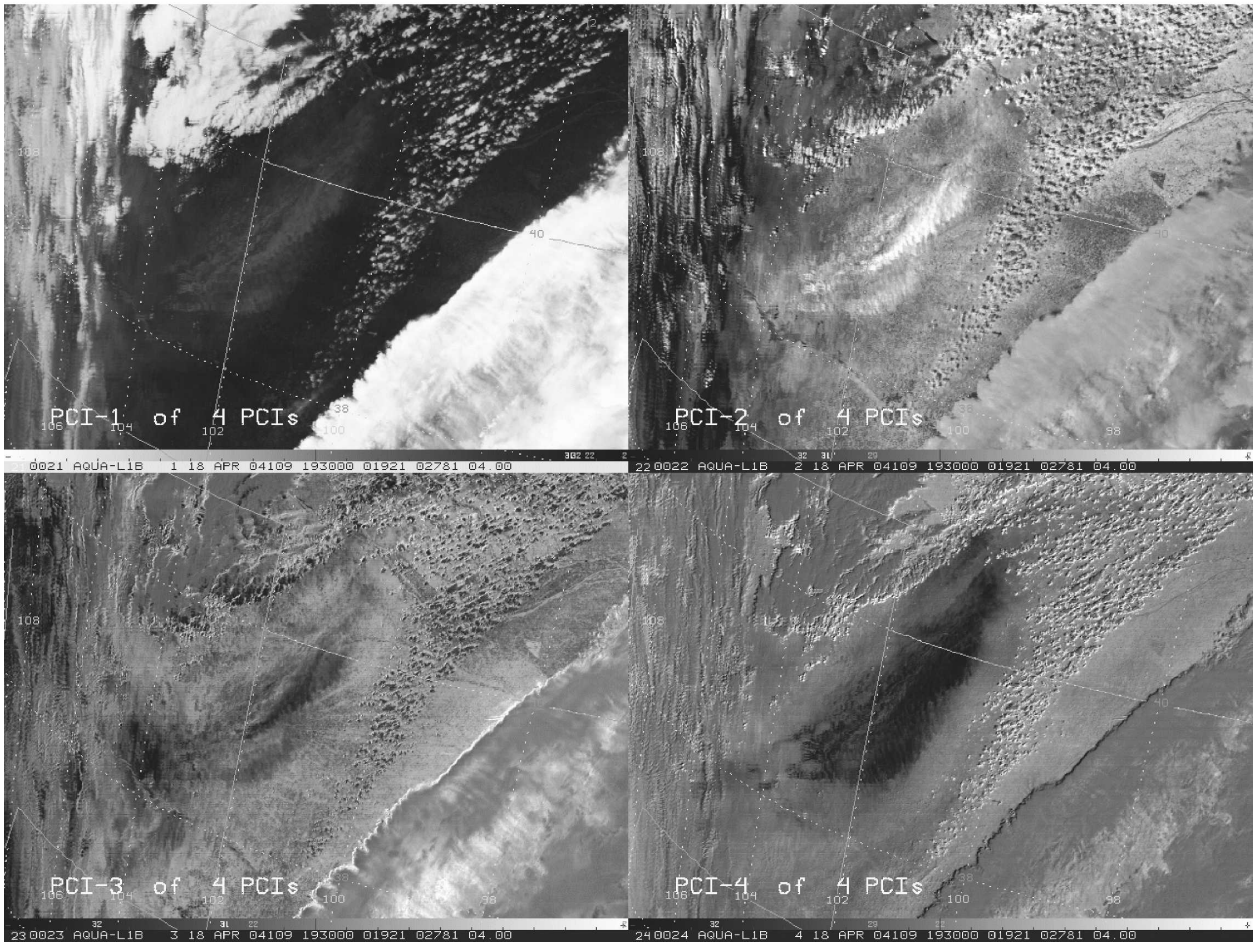

Fig. 6. (a) Four-panel image of four PCIs generated from ABI-equivalent MODIS bands at 3.9, 8.7, 10.8, and 12.0 μm, for the same case as in Figs. 3 and 4. (b) A plot of the MODIS band makeup of the four PCIs in (a). Other than the contribution of the additional band 22 (3.9 μm), note that the contributions of the other bands in PCI-1, -3, and -4 are similar to PCI-1, -2, and -3 in the three-band/three-PCI case in Fig. 5a. (c) Three-color blowing-dust product generated from PCI-2, -4, and -3 (red, green, and blue, respectively) in (a), showing dust as red, immediately surrounded by a clear-sky background in neutral color. The area near the source of the dust plume is orange. Clouds are represented by more neutral colors. Plotted winds represent the flow at the surface at the time of the image.

a bright red color, the features that originate and cover a large portion of the Texas Panhandle and follow the plotted winds, as well as move into western Oklahoma. The dust has a strong contrast to the fairly neutral colors for other image features, such as clear-sky and cloud features. As in the first case, plotted winds (magnitude and direction), representing the flow at surface observation locations at the time of the image, help verify the spatial extent and elongated orientation of the blowing dust.

Although both dust cases are daytime examples, the three-band/three-PCI analysis, which utilizes infrared spectral bands only with no reflected component, is expected to work similarly both day and night. Because the four-band/four-PCI version of this product will vary due to the reflected component of the shortwave band, the infrared-only three-band/three-PCI variation of the blowing-dust product may have to be used instead to provide a product that works better at night and does not change from day to night. This will be investigated with the real-time product loops that are planned.

Table 7 summarizes the three-color image combinations in the evolution of the new blowing-dust product as developed in the previous paragraphs. As with the new daytime fog/stratus product, the three-color blowing-dust product is currently being produced both day and night in real time from MSG imagery over West Africa on an experimental RAMSDIS unit at CIRA. As an example, a time series image loop of the three-color PCI blowing-dust product is available (online at

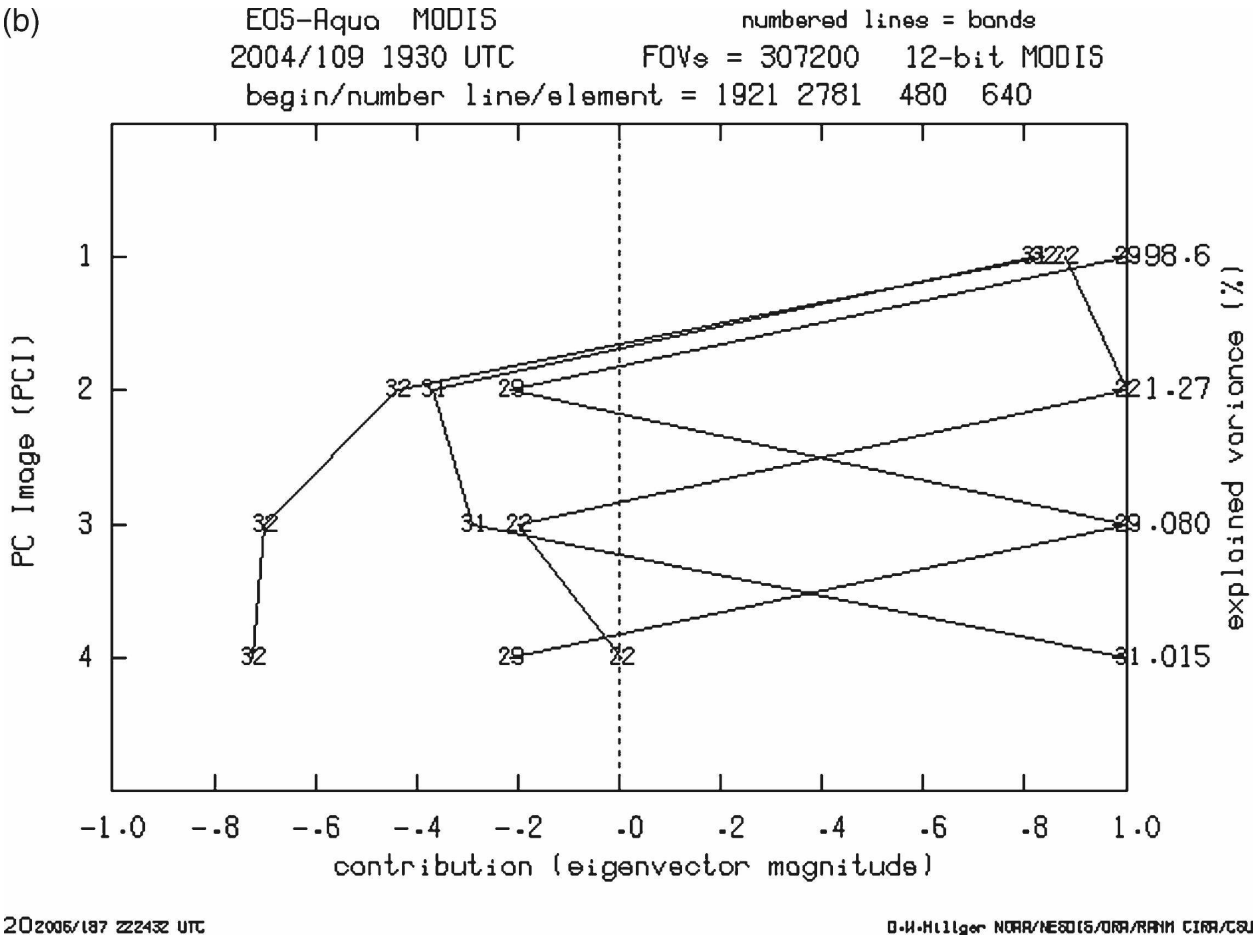

Fig. 6. (*Continued*)

http://rammb.cira.colostate.edu/intranet/Weeklies/Hillger060804/LoopDust/loop.html, which can be compared to the "Rosenfeld" dust product, online at http://rammb.cira.colostate.edu/intranet/Weeklies/Hillger060804/LoopRosen/loop.html).

In this example, the new three-color PCI dust product highlights the blowing dust more clearly than the product from which it was derived.

Another application of this product would be to improve detection of the Saharan air layer (SAL), which has been shown by Dunion and Velden (2004) to have a negative impact on Atlantic tropical cyclone activity. In the conclusion to their article, they were looking for ways to improve SAL detection and tracking.

4. Summary of methodology for color product development

In summary, based on the two new qualitative products presented as examples, the following factors were important in the selection of spectral bands used in product development for future implementation on GOES-R. Suggested methodologies include the following: 1) choose from among spectral bands equivalent to those that will be available on GOES-R ABI for future operational applications; 2) choose spectral bands that cover not only a wide range of the available spectrum, but those bands that cover the spectral regions known to be important for the features of interest; 3) choose spectral bands that are window bands for probing lower-atmospheric phenomena, when that is the region of interest; and 4) learn from, or leverage on, existing (past and present) products as a foundation for additional product improvements.

Also, if using PCIs to analyze the spectral bands: 1) avoid the lowest-order PCI (PCI-1), which contains a majority of the common/redundant information among the spectral bands in the analysis; 2) focus on higher-ordered PCI with spectral difference information; and 3) avoid very high-ordered PCIs, generated from all

(c)

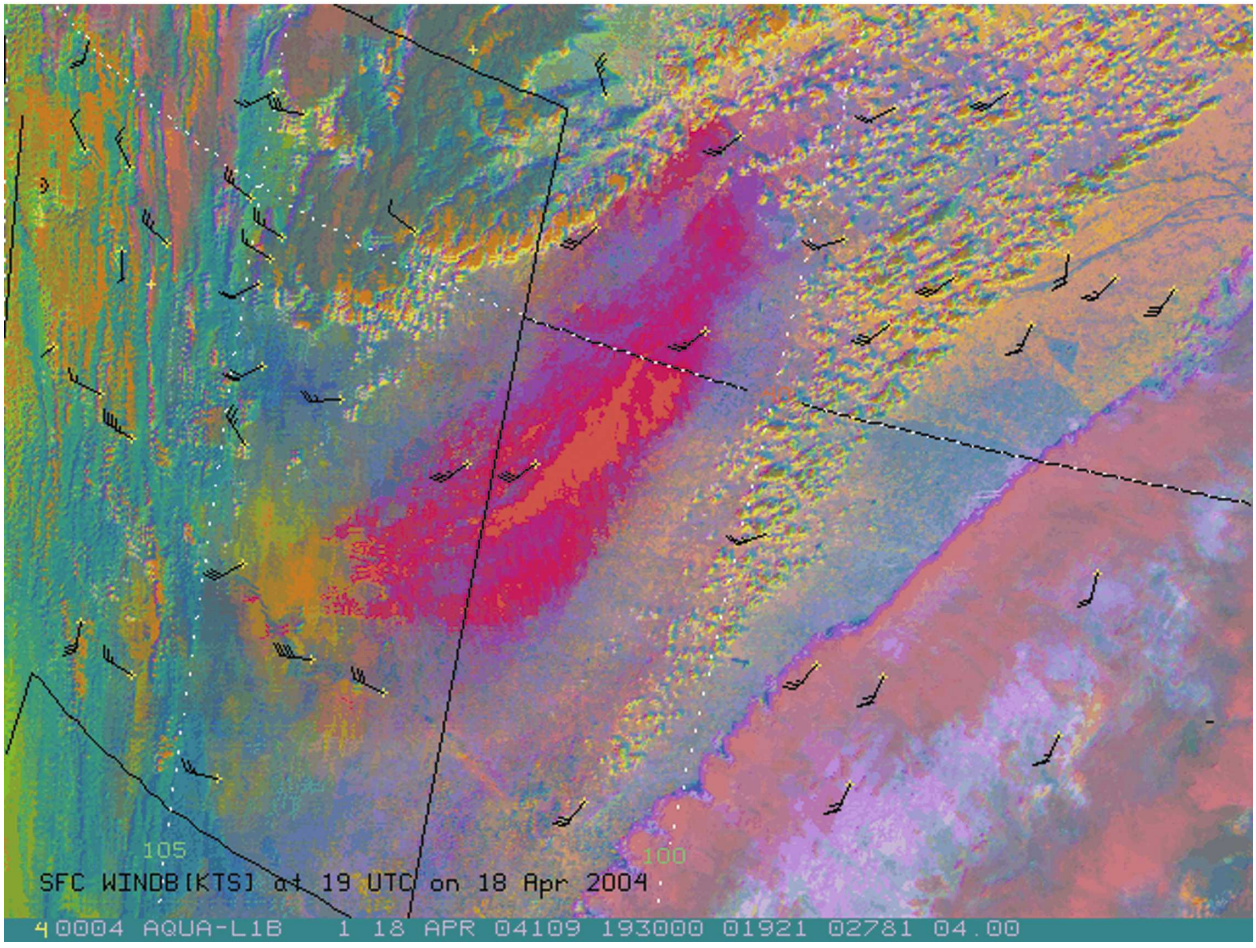

Fig. 6. (*Continued*)

available spectral bands, to minimize amplification of noise versus signal. This was found in previous applications of PCI analysis (Hillger and Clark 2002).

Also, in the *color* selection, it is important in the development of a three-color image product to choose 1) strongly contrasting colors for different image features, to discriminate the area of interest from other cloud and land surfaces (as in the daytime fog/stratus product); and 2) a bright color for detecting the feature of interest and fairly neutral colors if possible for the background, in contrast to the area of interest (as in the blowing-dust product).

(An important note: Even though a significant fraction of the population is color blind, that does not mean that these color products cannot be used. Colors can be quantized, and techniques are available to display colors that are considered significant as image masks, and to create products that can be used by those who would not benefit from the same product displayed using the colors described. This would also lead to more quantitative versions of these products, an area for future work.)

These guidelines proved helpful in new product development examples presented. Some of the choices of spectral bands and colors are partly a process of serendipity, because there are so many spectral bands available on existing experimental satellites and that will be available on future operational satellites. Yet those discoveries should be physically explainable, as seen in the analyses that were presented.

Often the atmospheric features that are desired (such as the examples presented for fog, stratus, and blowing dust) are sometimes poorly represented by conventional observations, so the image products created for these features usually show a much larger spatial extent and variability than can be verified. Some of these significant image features are "verified" only by temporal application (via image loop) of the new products to

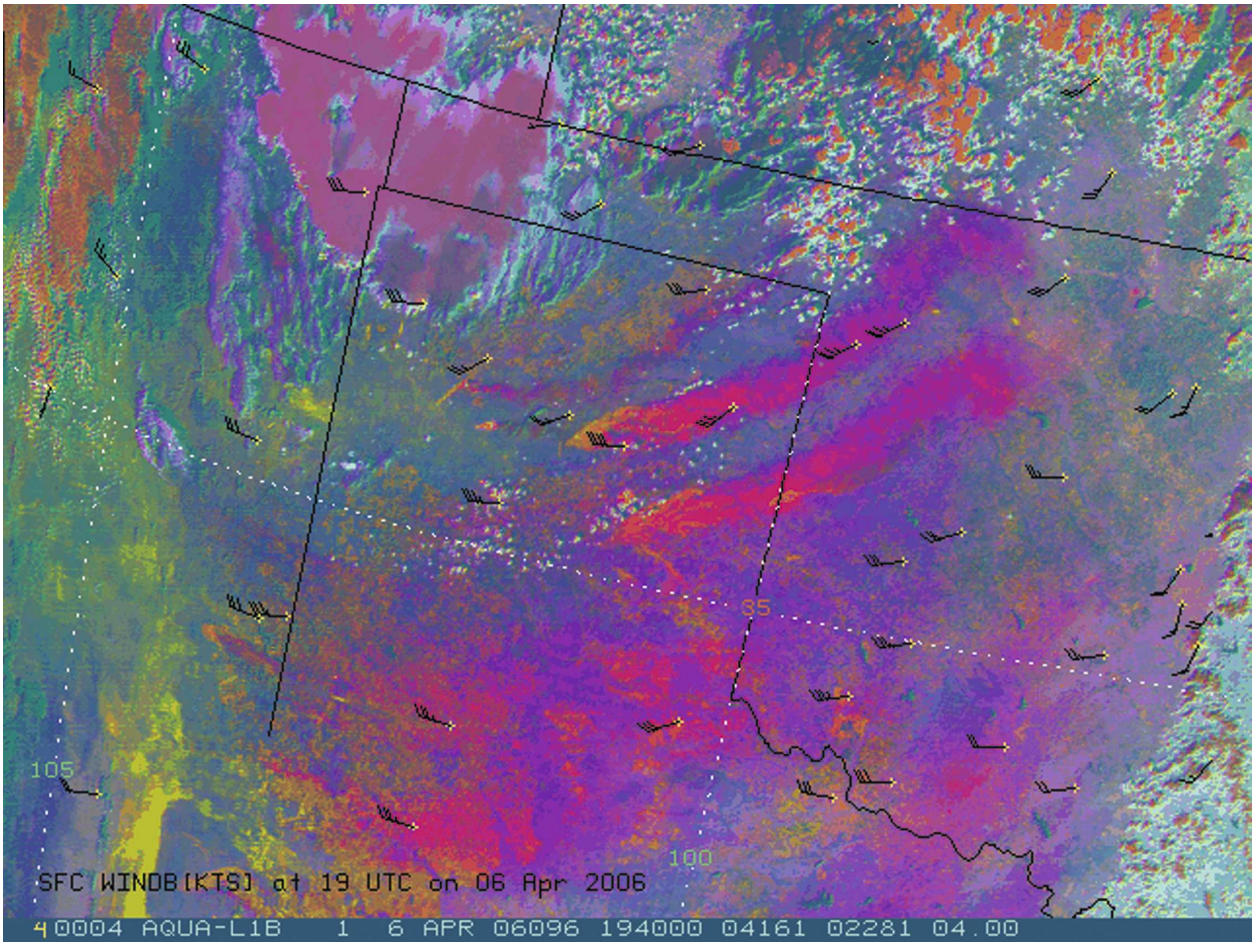

FIG. 7. Same as Fig. 6c, but for a second case of blowing dust in the Texas Panhandle and western Oklahoma at 1940 UTC 6 Apr 2006. Dust is again red, immediately surrounded by a relatively clear-sky background in neutral colors. Clouds are again represented by more neutral colors as well. Plotted winds represent the flow at the surface at the time of the image.

geostationary satellite data, such as those currently available with MSG. Readers are encouraged to view the image loops of these products (links provided above) to help assess their usefulness in view of the lack of supporting conventional observations at the much higher spatial resolution available with satellite imagery.

Both the daytime fog/stratus and blowing-dust products continue to be areas for future improvement. The development presented in this article is being implemented with real-time MSG data, with the color products soon to be available on the Web for users to view and evaluate, as opposed to the single examples of these product currently available in the links provided. As these products are generated in more and varied locations and times and are made available for public

TABLE 7. Summary of three-color image combinations for blowing dust detection/discrimination.

Three-color product name	Red component	Green component	Blue component	Image example
"Rosenfeld" three-color dust product	12.0–10.8 μm*	10.8–8.7 μm*	10.8 μm*	Fig. 4
Three-color blowing-dust product (8.7, 10.8, and 12.0 μm)	PCI-2 (of three PCIs)	PCI-3 (of three PCIs)	PCI-1 (of three PCIs)	Fig. 6c
Modified three-color blowing-dust product (adding 3.9 μm)	PCI-2 (of four PCIs)	PCI-4 (of four PCIs)	PCI-3 (of four PCIs)	Fig. 7b

* Special stretching/enhancements are applied to each difference or band image before combining.

distribution, as are many of the other MSG products that are provided for operational use by Eumetsat, they hopefully will continue to be found to correlate well with the limited spatial coverage of ground truth information (surface observations) that are available for verification, especially in many parts of the world with few meteorological observations. Comparison of the blowing-dust product can also be made directly with the Miller (2003) algorithm, as another form of verification, when the two products are produced for the same scenes.

The more subtle differences that are magnified by the three-color combinations, such as the ability to discriminate between fog (on or near the ground) and stratus (low- to middle-level cloud), resulting from differences in solar absorption and reflection that characterize these features, will be investigated in additional situations to quantify the difference between the two types of cloud, as was suggested by the scatterplots of image pixels that were utilized in section 2d. It is also possible that radiative transfer modeling of simulated dust cases, in particular, could help quantify the performance of these new image products.

With these two products as examples of the types of mesoscale services that can be available from future satellite instrumentation, the process continues with the development of other new and improved products for GOES-R. These efforts are part of the "risk reduction" activities being pursued in order to ensure that data from the GOES-R series will not go unused from the first day they are available. With the expense of satellite systems, it is important that the spatial, temporal, spectral, and radiometric improvements in GOES-R are utilized immediately when the first in the series of satellites is launched and declared operational.

Acknowledgments. Funding for this study is made available through NOAA Grant NA17RJ1228. The views, opinions, and findings contained in this article are those of the author and should not be construed as an official National Oceanic and Atmospheric Administration or U.S. government position, policy, or decision. The MODIS data for the cases used in this study were acquired as part of NASA's Earth Science Enterprise, archived and distributed by the Goddard Earth Sciences (GES) Data Information Services Center (DISC) Distributed Active Archive Center (DAAC). MSG data were captured from data servers that provide imagery for real-time use, operated by NOAA's Satellite Services Division (SSD). Some of the surface observations in McIDAS-compatible format were provided by the University of Wisconsin Space Science and Engineering Center (SSEC) Data Center thanks to Dee Wade.

APPENDIX

Three-Color Image Processing

Although the three-color image processing is fairly common in image analysis systems, there are limitations in the current version of Man Computer Interactive Data Access System (McIDAS)-based RAMSDIS (Molenar et al. 2000) used for the image analysis in this study. The McIDAS "combine" command creates a 24-bit three-color red–green–blue (RGB) display from three images designated as the red, green, and blue inputs. The RGB output can be turned into a JPG image, but cannot be saved as a McIDAS-formatted "AREA" file, limiting its usefulness for further display and looping within McIDAS. Therefore, as part of this effort, software has been written to create three-color McIDAS-formatted AREA files directly from the three (red, green, and blue) AREA files, emulating what is produced by using the McIDAS combine command, but with a more useful output.

The new software uses a FORTRAN algorithm coded by S. Q. Kidder (2006, personal communication), based on Heckbert's (1982) median cut algorithm. The Heckbert algorithm is called adaptive, tapered quantization, to reduce 24 bits of information (8 bits for each of three colors) to an 8-bit (256 color) final product. The algorithm involves the following three steps: 1) sampling the three original (red, green, and blue) images for color statistics, creating a color frequency histogram; 2) choosing a new color space based on the gathered statistics (The mean-cut algorithm does this by successively subdividing the color space so that each of the new colors is represented by an equal number of pixels from the original images. In this processing colors that are most widely used are saved and colors that are never or seldom used are eliminated.); and 3) mapping the original colors to the nearest neighbors in the new color space. At this point the colors are also sorted by their brightness or intensity to create a usable gray shade image should the color enhancement not be applied.

Although the algorithm can produce a 1 byte (8 bits) per pixel image, a modification was necessary for use in McIDAS. Because of the way graphics colors are interleaved with image colors within McIDAS, it was discovered that it was necessary to assign each color to two adjacent 8-bit values, reducing the number of available colors to only 7 bits (128 colors). This duplication of colors allows for pixels to shift by one count in the color table (when necessary to be compatible within McIDAS), showing the same color as intended and not a wrong color that could otherwise corrupt the final color image.

Output of the algorithm is an AREA file that can be displayed in a McIDAS frame or as a time series of images to be looped over multiple frames. A color enhancement is generated that is unique to each three-color AREA file that is produced. To have the proper three-color effect, that color enhancement needs to be applied to the corresponding image only. Therefore, when image loops are created, the three-color enhancement for each image needs to kept and applied to the intended image in the loop. The software developed for this image/enhancement matchup is used operationally to produce three-color images and time series loops of three-color images on several RAMSDIS units at CIRA.

REFERENCES

Ackerman, S. A., 1989: Using the radiative temperature difference at 3.7 and 11 micron to track dust outbreaks. *Remote Sens. Environ.,* **27,** 129–133.

——, 1997: Remote sensing aerosols using satellite infrared observations. *J. Geophys. Res.,* **102** (D14), 17 069–17 079.

Brindley, H. E., and J. E. Russell, 2006: Improving GERB scene identification using SEVIRI: Infrared dust detection strategy. *Remote Sens. Environ.,* **104,** 426–446.

d'Entremont, R. P., and L. W. Thomason, 1987: Interpreting meteorological satellite images using a color-composite technique. *Bull. Amer. Meteor. Soc.,* **68,** 762–768.

Dills, P. A., D. W. Hillger, and J. F. W. Purdom, 1996: Distinguishing between different meteorological phenomena and land surface properties using the multispectral imaging capabilities of GOES-8. Preprints, *Eighth Conf. on Satellite Meteorology and Oceanography,* Atlanta, GA, Amer. Meteor. Soc., 339–342.

Dunion, J. P., and C. S. Velden, 2004: The impact of the Saharan air layer on Atlantic tropical cyclone activity. *Bull. Amer. Meteor. Soc.,* **85,** 353–365.

Eastwood, S., and V. W. Thyness, 2003: Snow cover using 1.6 μm AVHRR channel 3A. *Proc. 2003 EUMETSAT Meteorological Satellite Conf.,* Weimar, Germany, EUMETSAT, 686–693.

Ellrod, G. P., 1995: Advances in the detection and analysis of fog at night using GOES multi-spectral infrared imagery. *Wea. Forecasting,* **10,** 606–619.

Heckbert, P., 1982: Color image quantization for frame buffer display. *ACM Comput. Graphics,* **16** (3), 297–307.

Hillger, D. W., and J. D. Clark, 2002: Principal component image analysis of MODIS for volcanic ash. Part I: Most important bands and implications for future GOES imagers. *J. Appl. Meteor.,* **41,** 985–1001.

——, and G. P. Ellrod, 2003: Detection of important atmospheric and surface features by employing principal component image transformation of GOES imagery. *J. Appl. Meteor.,* **42,** 611–629.

——, and M. DeMaria, 2007: GOES-R color product development. Preprints, *Third Symp. on Future National Operational Environmental Satellites,* San Antonio, TX, Amer. Meteor. Soc., P1.18. [Available online at http://ams.confex.com/ams/87ANNUAL/techprogram/paper_117094.htm.]

——, ——, and R. Zehr, 2004a: Advance mesoscale product development for GOES-R using operational and experimental satellite observations. *Weather and Environmental Satellites,* T. H. Vonder Haar and H.-L. Allen Huang, Eds., International Society for Optical Engineering (SPIE Proceedings Vol. 5549), 105–113.

——, ——, and J. Purdom, 2004b: Analysis of simulated GOES-R data and products for mesoscale meteorology. Preprints, *13th Conf. on Satellite Meteorology and Oceanography,* Norfolk, VA, Amer. Meteor. Soc., P1.8. [Available online at http://ams.confex.com/ams/pdfpapers/78966.pdf.]

——, ——, ——, and C. D. Barnet, 2004c: Risk reduction activities for future GOES-R instrumentation. *Fourth International Asia-Pacific Environmental Remote Sensing Symposium (Applications with Weather Satellites II),* W. P. Menzel and T. Iwasaki, Eds., International Society for Optical Engineering (SPIE Proceedings Vol. 5658), 66–74.

Kidder, S. Q., D. W. Hillger, A. J. Mostek, and K. J. Schrab, 2000: Two simple GOES Imager products for improved weather analysis and forecasting. *Natl. Wea. Dig.,* **24,** 25–30.

Miller, S. D., 2003: A consolidated technique for enhancing desert dust storms with MODIS. *Geophys. Res. Lett.,* **30,** 2071, doi:10.1029/2003GL018279.

Molenar, D. A., K. J. Schrab, and J. F. W. Purdom, 2000: RAMSDIS contributions to NOAA satellite data utilization. *Bull. Amer. Meteor. Soc.,* **81,** 1019–1030.

Rosenfeld, D., E. Cattani, S. Melani, and V. Levizzani, 2004: Considerations on daylight operation of 1.6 versus 3.7 μm channel on NOAA and METOP satellites. *Bull. Amer. Meteor. Soc.,* **85,** 873–881.

Strabala, K. I., S. A. Ackerman, and W. P. Menzel, 1994: Cloud properties inferred from 8-12 μm data. *J. Appl. Meteor.,* **33,** 212–229.